





# Genome Mosaicism in Field Strains of *Mycoplasma bovis* as Footprints of In-Host Horizontal Chromosomal Transfer

 Ana García-Galán,<sup>a</sup> Eric Baranowski,<sup>b</sup> Marie-Claude Hygonenq,<sup>b</sup> Mathilda Walch,<sup>b</sup> Guillaume Croville,<sup>b</sup> Christine Citti,<sup>b</sup> Christian De la Fe,<sup>a</sup>  Laurent-Xavier Nouvel<sup>b</sup>

<sup>a</sup>Ruminant Health Research Group, Department of Animal Health, Faculty of Veterinary Sciences, Regional Campus of International Excellence, "Campus Mare Nostrum," University of Murcia, Murcia, Spain

<sup>b</sup>IHAP, ENVT, INRAE, Université de Toulouse, Toulouse, France

**ABSTRACT** Horizontal gene transfer was long thought to be marginal in *Mollicutes*, but the capacity of some of these wall-less bacteria to exchange large chromosomal regions has been recently documented. *Mycoplasma* chromosomal transfer (MCT) is an unconventional mechanism that relies on the presence of a functional integrative conjugative element (ICE) in at least one partner and involves the horizontal acquisition of small and large chromosomal fragments from any part of the donor genome, which results in progenies composed of an infinite variety of mosaic genomes. The present study focuses on *Mycoplasma bovis*, an important pathogen of cattle responsible for major economic losses worldwide. By combining phylogenetic tree reconstructions and detailed comparative genome analyses of 36 isolates collected in Spain (2016 to 2018), we confirmed the mosaic nature of 16 field isolates and mapped chromosomal transfers exchanged between their hypothetical ancestors. This study provides evidence that MCT can take place in the field, most likely during coinfections by multiple strains. Because mobile genetic elements (MGEs) are classical contributors of genome plasticity, the presence of phages, insertion sequences (ISs), and ICEs was also investigated. Data revealed that these elements are widespread within the *M. bovis* species and evidenced classical horizontal transfer of phages and ICEs in addition to MCT. These events contribute to wide-genome diversity and reorganization within this species and may have a tremendous impact on diagnostic and disease control.

**IMPORTANCE** *Mycoplasma bovis* is a major pathogen of cattle that has significant detrimental effects on economics and animal welfare in cattle rearing worldwide. Understanding the evolution and the adaptative potential of pathogenic mycoplasma species in the natural host is essential to combating them. In this study, we documented the occurrence of mycoplasma chromosomal transfer, an atypical mechanism of horizontal gene transfer, in field isolates of *M. bovis* that provide new insights into the evolution of this pathogenic species in their natural host. Although these events are expected to occur at low frequency, their impact is accountable for genome-wide variety and reorganization within *M. bovis* species, which may compromise both diagnostic and disease control.

**KEYWORDS** *Mycoplasma bovis*, horizontal gene transfer, mosaic genomes, mobile genetic elements, *Mycoplasma* chromosomal transfer

Horizontal gene transfer (HGT) has deeply influenced our perception of bacterial evolution. By allowing the exchange of genetic material between organisms that are not in a parent-offspring relationship, HGT endows bacteria with the ability to eliminate deleterious mutations, respond to rapid environmental changes, and explore new ecological niches (1). Until recently, HGT was thought to be marginal in mycoplasmas (class *Mollicutes*), a large group of wall-less bacteria often portrayed as minimal cells because of their reduced genomes (ca. 0.5 to 2.0 Mb) and limited metabolic pathways (2). Indeed, genome erosion—a

**Citation** García-Galán A, Baranowski E, Hygonenq M-C, Walch M, Croville G, Citti C, De la Fe C, Nouvel L-X. 2022. Genome mosaicism in field strains of *Mycoplasma bovis* as footprints of in-host horizontal chromosomal transfer. *Appl Environ Microbiol* 88:e01661-21. <https://doi.org/10.1128/AEM.01661-21>.

**Editor** Maia Kivisaar, University of Tartu

**Copyright** © 2022 American Society for Microbiology. All Rights Reserved.

Address correspondence to Laurent-Xavier Nouvel, [xavier.nouvel@envt.fr](mailto:xavier.nouvel@envt.fr).

**Received** 18 August 2021

**Accepted** 9 October 2021

**Accepted manuscript posted online** 20 October 2021

**Published** 11 January 2022

degenerative process resulting from successive losses of genetic materials—was long considered the only force driving the evolution of *Mollicutes* from their Gram-positive ancestors (3). Recent evidence of massive HGT in *Mycoplasma* and other genera of the class *Mollicutes*, such as *Ureaplasma* or *Spiroplasma*, have provided a new frame to understand the evolution of these minimal bacteria (4–11). HGT in ruminant mycoplasmas was first documented by comparative genomic studies that have revealed the exchanges of large chromosomal regions between phylogenetically remote species known to share the same ecological niche (6). These data were further supported by the identification of integrative conjugative elements (ICE) in the genome of several ruminant mycoplasma species and the demonstration that these mobile genetic elements (MGEs) were able to confer conjugative properties to their recipient strains (12, 13). Mycoplasma ICEs belong to a new family of transmissible elements that encode the machinery for their self-excision, transmission by conjugation, and random integration into the genome of the recipient cell, where they replicate as part of the host chromosome (11). Remarkably, ICEs were also found to play a key role in mycoplasma chromosomal transfer (MCT), an unconventional mechanism of HGT that involves the horizontal acquisition of small and large chromosomal fragments originating from any part of the donor genome. This distributive process results in replacing several regions of the recipient chromosome at homologous sites (14) and offers these minimal bacteria a remarkable adaptive potential by generating a complex progeny consisting of an almost infinite variety of mosaic genomes (15, 16). A broad distribution of ICEs is observed among ruminant mycoplasmas, with two types circulating within phylogenetically distant species (17). The widespread occurrence of ICEs in ruminant mycoplasmas, together with their capacity to promote conjugation, which in turn allows MCT, raises questions regarding the potential emergence of mosaic genomes in the field.

The present study focuses on *Mycoplasma bovis*, a cattle pathogen that induces major economic impacts on the global livestock industry and causes mastitis, arthritis, pneumonia, keratoconjunctivitis, otitis media, and genital disorders (18, 19). The spread of *M. bovis* infection among animals, herds, regions, or countries is usually associated with animal movements and the introduction of asymptomatic carriers, which are occasionally shedding the pathogen in milk, colostrum, nasal, or genital secretions (18–20). A recent molecular typing of *M. bovis* strains circulating in Spain revealed two subtypes (STs), both being found in beef and dairy cattle, regardless of regions and clinical signs (21). Remarkably, several animals were found to be concomitantly infected by two *M. bovis* genotypes revealing a favorable epidemiological context for MCT in this pathogenic species. This particular context led us to investigate the occurrence of mosaic genomes among *M. bovis* isolates collected in Spain between 2016 and 2018 by whole-genome sequencing. Phylogenetic tree reconstructions based on multilocus sequence typing (MLST) and whole-genome sequence-single nucleotide polymorphism (WGS-SNP) revealed several discrepancies pointing toward mosaic genomes. Detailed comparative genomic analyses further confirmed the mosaic nature of these genomes and precisely mapped chromosomal fragments that had been exchanged between their hypothetical ancestors.

## RESULTS

***M. bovis* genotypes circulating in Spain are globally distributed.** A coarse-grained image of *M. bovis* genotypes circulating in Spain has been generated by single-locus typing using *polC* sequences (21, 22). Here, isolates belonging to *polC*-ST2 ( $n = 16$ ) and *polC*-ST3 ( $n = 20$ ) were further sequenced by Illumina technology, characterized by two MLST schemes (23, 24) and WGS-SNP genotyping (Table 1). These data were combined with those available for MLST-2 in the PubMLST database (<https://pubmlst.org/organisms/mycoplasma-bovis>) to study the global population structure of *M. bovis*. The minimum spanning tree (MST) generated failed to reveal any correlation between a geographic origin and a particular ST (Fig. 1). Indeed, most lineages, with more than one isolate, included members from different countries or even different continents. Several notable exceptions included STs detected only in Canada (e.g., ST65), Israel (e.g., ST33), the United States (e.g., ST15), China (e.g., ST90), and Japan (e.g., ST100). However, this apparent correlation is weak considering

**TABLE 1** Epidemiological background, molecular characterization, and mobilome composition of *M. bovis* isolates included in the study

Isolate	Sample source	Year	Farm region	Enrofloxacin MIC	po/C-ST	Molecular typing <sup>b</sup>				WGS-SNP <sup>f</sup>	ISs <sup>c</sup>	MAGv1-like phage <sup>d</sup>				ICE backbone CDSs <sup>e</sup>				
						MLST-1	MLST-2	MLST-1	MLST-2			Transposases	Locus I: 536074	Locus II: 548254	Locus III: 911138	I	II	III	IV	
PG45	Mastitic milk	1961	CO	0.125	1	1	12	m		+	(54)	-	-	-	-	-	-	-	-	-
J69	Auricular <sup>1</sup>	2016	VC <sup>5</sup>	16	3	8	21	a		+		Vestige	-	Complete	*	*	*	*	*	*
J72	Lung <sup>1</sup>	2016	VC <sup>5</sup>	16	3	8	21	a		+		Vestige	-	Complete	*	*	*	*	*	*
<b>J81</b>	<b>Nasal</b>	<b>2016</b>	<b>RM<sup>6</sup></b>	<b>16</b>	<b>3</b>	<b>8</b>	<b>21</b>	<b>a</b>		+	(70)	<b>Vestige</b>	-	<b>Complete</b>	*	*	*	*	*	*
J115	Auricular	2016	VC <sup>7</sup>	16	3	8	21	a		+		Vestige	-	Complete	*	*	*	*	*	*
J131	Auricular	2017	RM <sup>6</sup>	16	3	8	21	a		+		Vestige	-	Complete	*	*	*	*	*	*
<b>J228</b>	<b>Lung</b>	<b>2017</b>	<b>RM<sup>9</sup></b>	<b>1</b>	<b>3</b>	<b>59</b>	<b>129</b>	<b>b</b>		+	(69)	<b>Vestige</b>	-	<b>Complete</b>	*	*	*	*	*	*
<b>J279</b>	<b>Nasal</b>	<b>2017</b>	<b>CL<sup>10</sup></b>	<b>2</b>	<b>3</b>	<b>59</b>	<b>129</b>	<b>b</b>		+	(69)	<b>Vestige</b>	-	<b>Complete</b>	*	*	*	*	*	*
<b>J137</b>	<b>Nasal<sup>2</sup></b>	<b>2017</b>	<b>RM<sup>8</sup></b>	<b>0.5</b>	<b>2</b>	<b>8</b>	<b>96</b>	<b>c</b>		+	(80)	<b>Truncated<sup>23</sup></b>	-	-	*	*	*	*	*	*
J28	Nasal	2016	VC <sup>11</sup>	16	3	61	21	d		+		Vestige	-	Vestige	*	*	*	*	*	*
J403	Mastitic milk	2017	C <sup>12</sup>	<0.0625	3	8	21	e		+		Vestige	-	Vestige	*	*	*	*	*	*
J414	Mastitic milk	2017	C <sup>12</sup>	<0.0625	3	8	21	e		+		Vestige	-	Vestige	*	*	*	*	*	*
J433	Nasal	2018	E <sup>13</sup>	0.125	3	8	21	e		+		Vestige	-	Vestige	*	*	*	*	*	*
J335	Nasal <sup>3</sup>	2017	RM <sup>14</sup>	<0.0625	3	60	122	f		+		Vestige	-	Vestige	*	*	*	*	*	*
J479	Nasal	2018	RM <sup>15</sup>	32	3	7	128	g		+		Vestige	-	Complete	*	*	*	*	*	*
J482	Lung	2018	RM <sup>15</sup>	32	3	7	128	g		+		Vestige	-	Complete	*	*	*	*	*	*
J96	Spleen <sup>4</sup>	2016	VC <sup>16</sup>	16	3	8	130	h		+		Vestige	-	Vestige	*	*	*	*	*	*
J388	Nasal	2017	VC <sup>11</sup>	32	3	8	122	i		+		Vestige	-	Vestige	*	*	*	*	*	*
J233	Nasal	2017	VC <sup>17</sup>	32	3	8	122	j		+		Truncated <sup>24</sup>	-	-	*	*	*	*	*	*
J295	Nasal	2017	CL <sup>10</sup>	32	3	8	122	j		+		Truncated <sup>24</sup>	-	-	*	*	*	*	*	*
J305	Nasal	2017	CL <sup>10</sup>	16	3	8	122	j		+		Truncated <sup>24</sup>	-	-	*	*	*	*	*	*
J178	Nasal	2017	RM <sup>18</sup>	16	3	8	122	k		+		Vestige	-	Vestige	*	*	*	*	*	*
J391	Nasal	2017	VC <sup>11</sup>	0.5	2	53	8	l		+		-	-	*	*	*	*	*	*	*
J410	Mastitic milk	2017	C <sup>12</sup>	0.5	2	53	8	l		+		-	-	*	*	*	*	*	*	*
<b>J6</b>	<b>Nasal</b>	<b>2016</b>	<b>VC<sup>11</sup></b>	<b>0.25</b>	<b>2</b>	<b>53</b>	<b>8</b>	<b>l</b>		+	(52)	<b>Complete</b>	-	-	*	*	*	*	*	*
J103	Lung <sup>4</sup>	2016	VC <sup>16</sup>	0.25	2	53	8	l		+		Complete	-	-	*	*	*	*	*	*
J136	Auricular <sup>2</sup>	2017	RM <sup>8</sup>	0.5	2	53	8	l		+		Complete	-	-	*	*	*	*	*	*
J175	Nasal	2017	RM <sup>18</sup>	0.25	2	53	8	l		+		Complete	-	-	*	*	*	*	*	*
J226	Lung	2017	RM <sup>19</sup>	0.25	2	53	8	l		+		Complete	-	-	*	*	*	*	*	*
J276	Nasal	2017	CL <sup>10</sup>	0.25	2	53	8	l		+		Complete	-	-	*	*	*	*	*	*
J319	Mastitic milk	2017	CM <sup>20</sup>	0.25	2	53	8	l		+		Complete	-	-	*	*	*	*	*	*
J330	Nasal	2017	RM <sup>14</sup>	0.25	2	53	8	l		+		Complete	-	-	*	*	*	*	*	*
J336	Nasal <sup>3</sup>	2017	RM <sup>14</sup>	0.25	2	53	8	l		+		Complete	-	-	*	*	*	*	*	*
J341	Nasal	2017	RM <sup>14</sup>	0.125	2	53	8	l		+		Complete	-	-	*	*	*	*	*	*
J356	Nasal	2017	RM <sup>21</sup>	0.25	2	53	8	l		+		Complete	-	-	*	*	*	*	*	*
J368	Nasal	2017	RM <sup>22</sup>	0.5	2	53	8	l		+		Complete	-	-	*	*	*	*	*	*
J377	Nasal	2017	RM <sup>22</sup>	0.5	2	53	8	l		+		Complete	-	-	*	*	*	*	*	*

<sup>a</sup>Background information was retrieved from previous studies (21, 58). Superscripts 1 to 4 designate samples collected from the same animal. Superscripts 5 to 22 were used to identify farms in each region. CO, Connecticut; VC, Valencian Community; RM, Region of Murcia; CL, Castile and León; CM, Castile-La Mancha; C, Catalonia; E, Extremadura.

<sup>b</sup>The subtype (ST) numbers are given according to previously developed typing systems (22–24). For multilocus sequence type 1 (MLST-1), new STs are underlined and given according to those defined previously (23, 39, 52). The letters (a to m) are given according to the phylogenetic tree obtained by WGS-SNP.

<sup>c</sup>For PG45, the number of transposases is given as previously reported (30). In the Spanish strains with circularized genomes (indicated in bold), the total number of transposases is indicated in parentheses. IS, insertion sequence. + indicates at least one complete transposase, and # indicates at least one pseudogene of transposase.

<sup>d</sup>The numbers indicate PG45 genomic positions corresponding to MAGv1-like phage insertion in *M. bovis* isolates. Position 911138 is approximate because determining the exact MAGv1-like insertion site was not possible given the occurrence of an IS. Superscripts 23 and 24 indicate that the MAGv1-like phage is truncated in the right and the left side (5' to 3'), respectively. For complete, vestigial and truncated phages see Fig. 5.

<sup>e</sup>Integrative conjugative element (ICE) backbone coding DNA sequences (CDSs) 1, 3, 5, 14, 16, 17, 19, and 22 as previously described (11). \* indicates the presence of CDSs, and - indicates the absence of CDSs.

<sup>f</sup>WGS-SNP, whole-genome sequence-single nucleotide polymorphism.

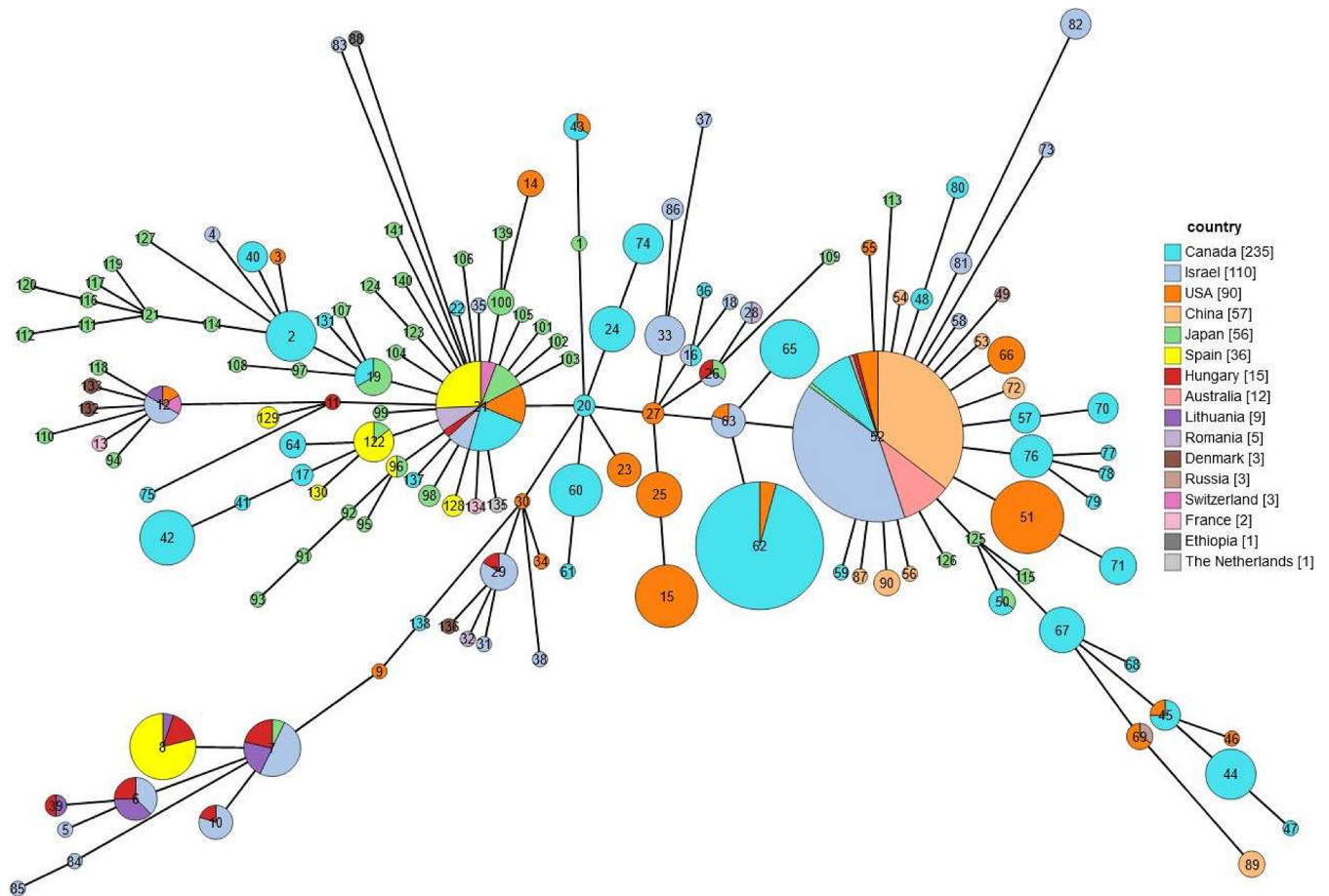


**FIG 1** Global distribution of worldwide isolates using MLST-2 typing. MST representing the global distribution of the PubMLST STs (MLST-2) thus far defined for *M. bovis* as of January 2020 and found among the isolates publicly available in the database and with an assigned ST (<https://pubmlst.org/organisms/mycoplasma-bovis>). Each circle represents a unique ST indicated with a number. Circles or portions thereof are sized in proportion to the number of isolates of each ST and are colored to indicate the country where they were found. In the legend, the number of isolates of each country is indicated in brackets. The 36 Spanish isolates are colored in yellow. The tree was created with GrapeTree (55).

that those countries are the source of most isolates available in the database. In Spain, four of the seven STs identified, namely, ST8, ST21, ST96, and ST122, have also been detected in other countries. These data suggest an efficient circulation of *M. bovis* between countries and even between continents.

**Identification of *M. bovis* isolates with a complex phylogenetic origin.** Phylogenetic analyses based on selected loci versus whole-genomic data revealed slightly different outcomes depending on the typing system (Table 1). MLST-1 identified seven STs, with the Spanish isolates clustering into three main branches (Table 1 and Fig. S1). In contrast to most *polC*-ST2 isolates (15 of 16) that clustered into a single ST53, *polC*-ST3 isolates were found scattered into five STs and two main branches. One of these branches includes only two isolates (J228 and J279) belonging to ST59, which shares four alleles (*dnaA*, *recA*, *tufA*, and *tkt*) with the reference strain PG45. Remarkably, one *polC*-ST2 isolate (J137) was classified into ST8, which mainly includes *polC*-ST3 isolates. The data generated with MLST-2 were consistent with MLST-1 (Table 1 and Fig. 2), with only minor differences in the clustering of *polC*-ST3 isolates. These data confirm the proximity of J228 and J279 with PG45, which share four identical alleles (*dnaA*, *glxX*, *gyrB*, and *tkt*), as well as the clustering of J137 with *polC*-ST3 isolates. The phylogenetic analysis based on WGS-SNP genotyping grouped Spanish isolates into two main branches: (i) branch A encompassing STs a to k and (ii) branch B composed only of ST l (Table 1 and Fig. 3). As expected, this system was highly discriminative, with up to 10 STs identified for *polC*-ST3 isolates in branch A and two for *polC*-ST2 isolates, one of them being J137 (ST c) that clustered together with *polC*-ST3 isolates (Fig. 3). Finally, J228

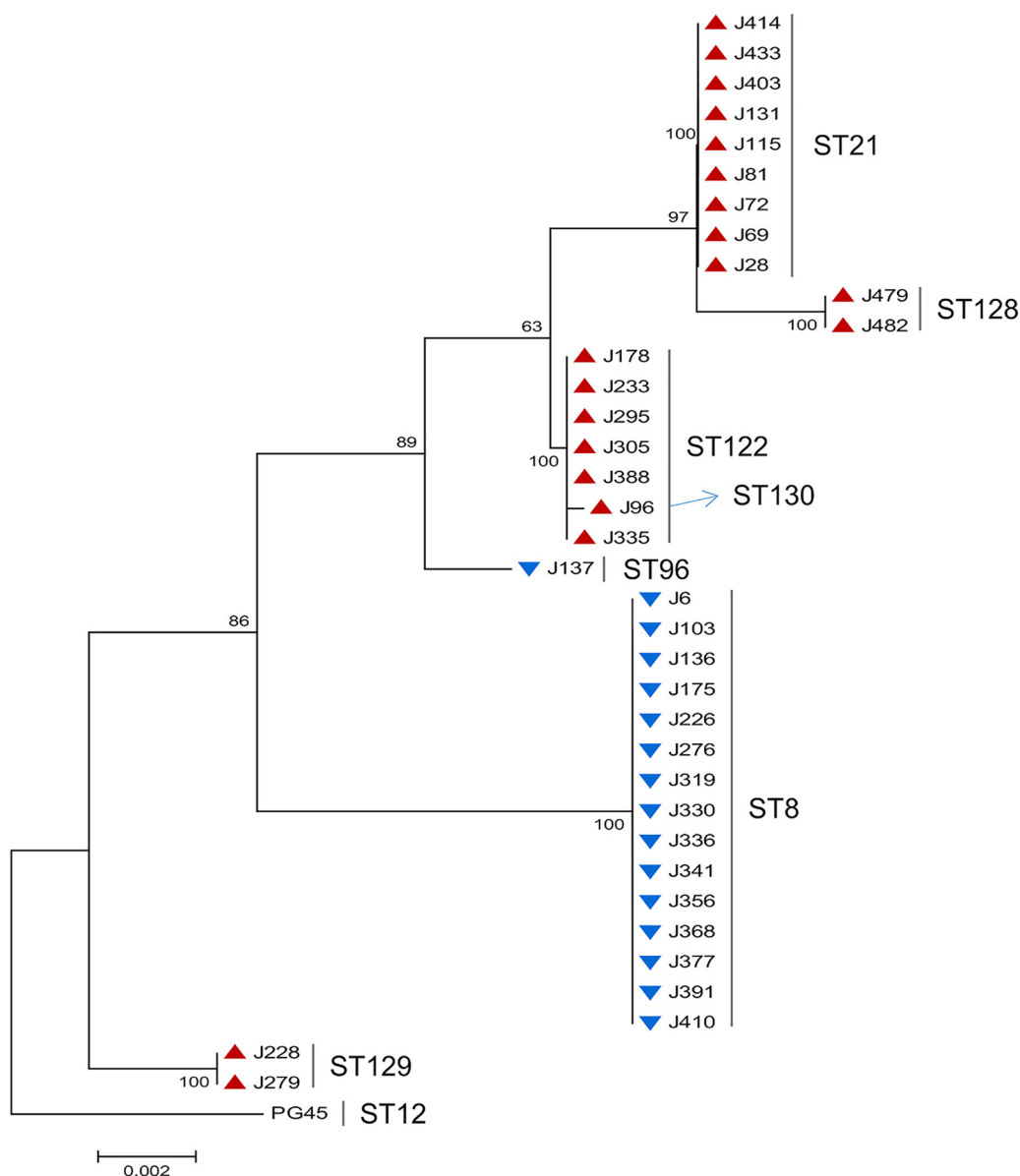


**FIG 2** Molecular phylogenetic analysis based on MLST-2 concatenated sequences. Phylogenetic tree inferred from the concatenated partial sequences of the seven genes included in the MLST-2 and corresponding to 36 *M. bovis* field isolates and the reference strain PG45 (CP002188.1). The red triangles refer to *poIC*-ST3 isolates, and the blue triangles refer to *poIC*-ST2 isolates. The tree was constructed by using the neighbor-joining method, the Tamura-Nei genetic distance model, and 1,000 bootstrap replicate analyses. Evolutionary analyses were conducted in MEGA X (51).

and J279 were found to cluster in branch A, together with the other *poIC*-ST3 isolates. No correlation was found between the occurrence of a particular ST and the sample source, year of isolation, or origin of the isolates in none of the three systems (Table 1). Overall, the three typing systems provide similar results showing two groups of isolates: one with a low diversity level (corresponding to *poIC*-ST2 isolates) and one with higher heterogeneity (corresponding to *poIC*-ST3 isolates). Remarkably, all molecular typing systems pointed toward three isolates, namely, J137, J228 and J279, the phylogenetic classification of which was inconsistent. Nanopore sequencing combined with Illumina permitted circularized genomes to be obtained for these isolates (Fig. 4). Genome analyses further showed that J228 and J279 are nearly identical (Data Set S1), with J279 having one additional coding DNA sequence (CDS) belonging to a family of lipoproteins, the DUF285 or PARCEL family, known to vary in gene number and expression within the species (25) compared to J228. Below,

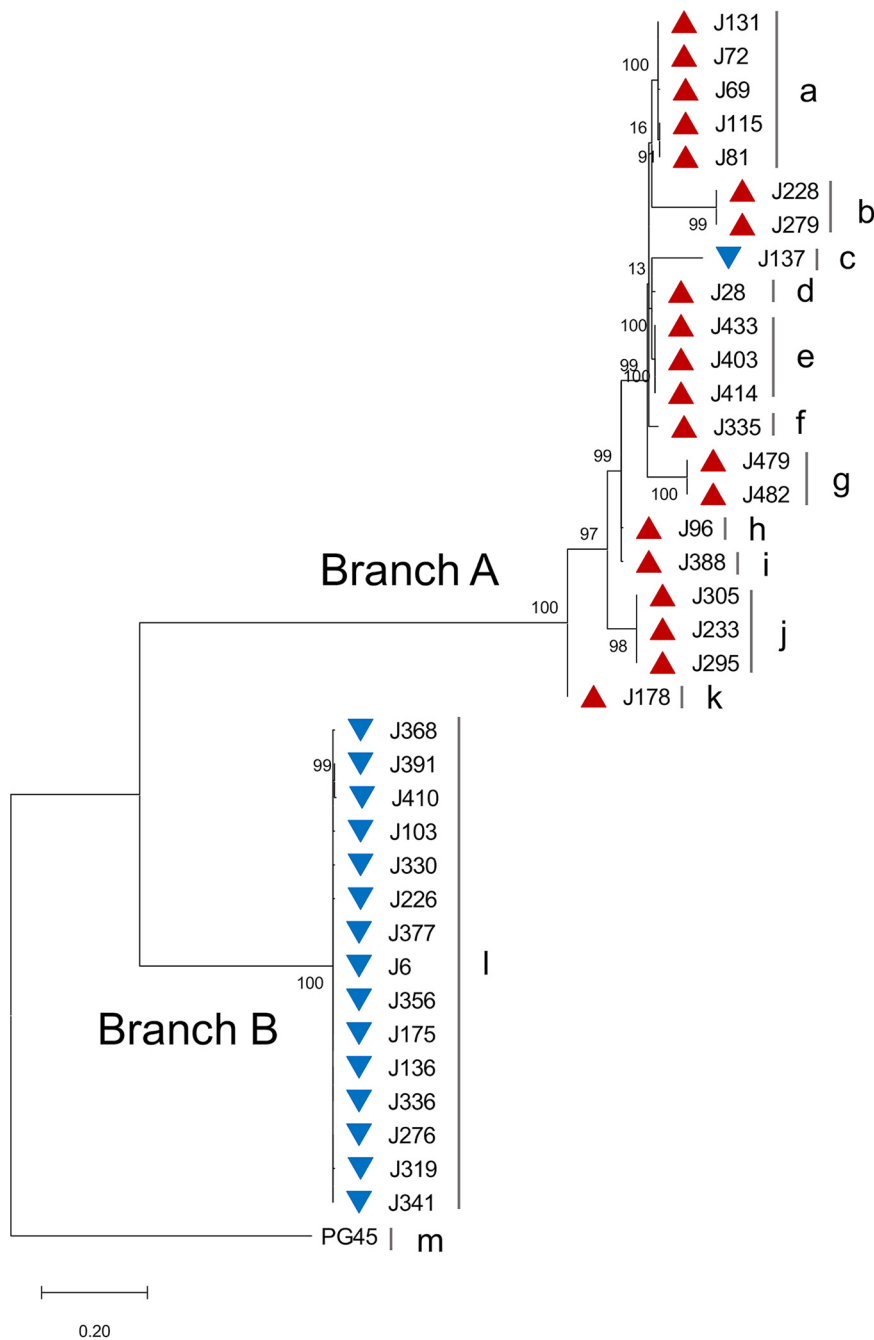


**FIG 3** WGS-SNP-based phylogenetic analysis of 36 *M. bovis* field isolates in comparison to the reference strain PG45. The red triangles refer to *polC*-ST3 isolates, and the blue triangles refer to *polC*-ST2 isolates. The tree was constructed by using the maximum likelihood method, the Tamura-Nei genetic distance model, and 1,000 bootstrap replicate analyses. Evolutionary analyses were conducted in MEGA X (51).

we sometimes refer to these isolates as J228/279, keeping in mind this difference and that they were isolated from two distinct geographic areas in the same year.

**MGEs are widespread among field strains.** Because MGEs are known as the main contributors of genome plasticity, the presence of phages, insertion sequences (ISs), and ICEs was investigated in the set of 36 Spanish isolates. A MAgV1-like prophage, initially described in *Mycoplasma agalactiae* (26) but absent from *M. bovis* type strain PG45, was recently identified in the French *M. bovis* isolate RM16 (27, 28). Homologous MAgV1-like sequences were found in all the Spanish strains except for two, J391 and J410, belonging to



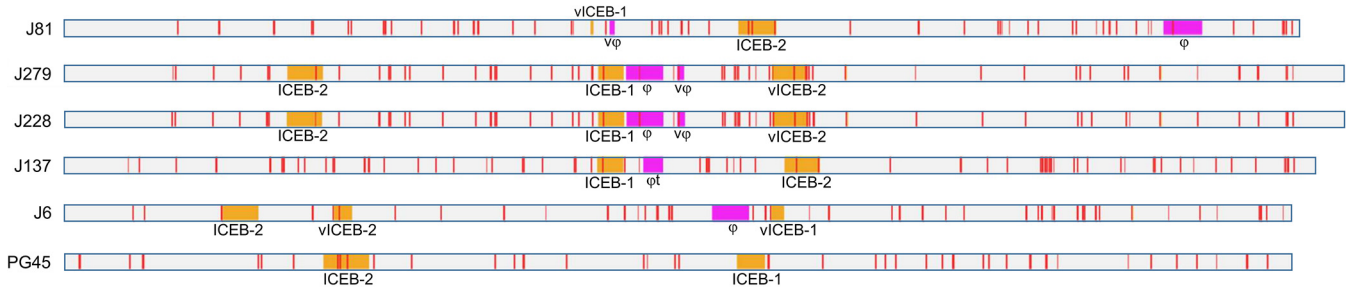


**FIG 4** MGE genomic distribution among *M. bovis* genomes circularized in this study and reference strain PG45. DNAPlotter linear representation of the genome circularized assemblies obtained with Oxford nanopore and Illumina sequencing data (see Materials and Methods). ISs, MAgV1-like sequences, and integrative conjugative elements (ICEs) are indicated in red, pink, and orange, respectively. ICE vestiges (vICEB) composed of less than two CDSs are not visualized but are described in Fig. S3.

branch B (Table 1). More specifically, in branch B, prophage-positive strains all displayed a complete MAgV1-like version inserted at the same position (locus I, nucleotide 536074 in PG45), whereas branch A strains harbor only vestigial or truncated prophage versions at this position (Table 1), with some ( $n = 9$ ) displaying a complete prophage copy at a distinct locus (locus II, PG45 nucleotide 548254; locus III, PG45 nucleotide 911138). These findings, when superimposed on the phylogenetic history, suggest that branch A underwent two events: phage erosion leading to truncated or vestigial forms at locus 1 and independent episodes of phage attack at different loci (Table 1).

The overall genetic organization of the MAgV1-like prophage was compared in circularized genomes (J6, J81, J137, J228, and J279) using *M. bovis* RM16 as a reference (Fig. 5). The number of CDSs and their orientation and size were highly similar to that found in RM16, the only differences being the occurrence of the IS element *ISMbov4* in J81, J228, and J279. These strains also carried either prophage vestiges composed of a few CDSs (J81, J228, and J279) or truncated versions corresponding to about half of the prophage (J137) (Fig. 5).

IS elements were identified in all Spanish isolates based on sequence similarities with transposases referenced in the ISFinder database (29) (Table 1). Between 52 and

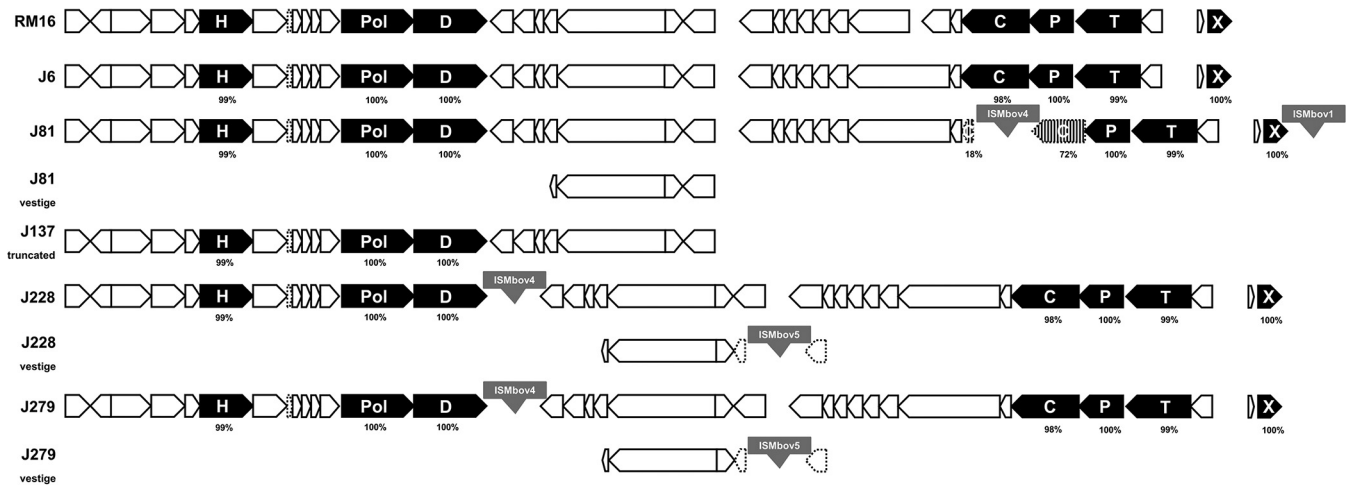


**FIG 5** Comparison of complete, vestigial, and truncated MAgV1-like phages with that identified in the circular *M. bovis* RM16 genome. The locations and orientations of the CDSs are indicated by arrows. CDSs highly conserved across MAgV1-like phages identified across mycoplasma species are shaded in black (26, 27). The letter codes in black arrows refer to: H, helicase; Pol, DNA polymerase; D, DNA primase; C, prohead protein; P, portal; T, terminase; X, Xer. For each shaded CDS, the percentage of global similarity with MAgV1-like identified in RM16 was calculated by using the EMBOSS Needle alignment tool, and it is indicated under the arrow (59). ISs are represented by gray boxes and are named according to the ISFinder database (29). CDSs interrupted by an IS are represented as pseudogenes with hatched colors and/or with dotted lines. Truncated phages refer to a region displaying only a part of the phage but containing the conserved polymerase, helicase, and DNA primase genes. Vestigial forms contained none of these genes and are reduced to very few predicted CDSs. MAgV1-like genomic positions and sizes are: RM16, positions 500818 to 532597 and 31.7 kb; J6, positions 548229 to 580006 and 31.7 kb; J81, complement (positions 937518 to 970642) and 33.1 kb; J81<sub>vestigier</sub> complement (positions 464793 to 469404) and 4.6 kb; J137<sub>truncated</sub> complement (positions 503457 to 521011) and 17.5 kb; J228, positions 500615 to 533739 and 33.1 kb; J228<sub>vestigier</sub> complement (positions 546225 to 552494) and 6.2 kb; J279, positions 500599 to 533723 and 33.1 kb; J279<sub>vestigier</sub> complement (positions 546209 to 552478) and 6.2 kb.

80 transposases were identified in strains with circularized genomes (Table 1 and Fig. 4). No correlation was found between the presence and/or the number of transposases and the epidemiological background or phylogenetic history of each strain.

Finally, particular attention was dedicated to ICEs, which are required for conjugation and MCT (11, 14). Their occurrence was determined by BLASTn using the two ICE sequences of the PG45 type strain, namely, ICEB-1<sub>PG45</sub> and ICEB-2<sub>PG45</sub> (11, 30). Results showed that the Spanish isolates all possess at least one CDS of ICEB having a minimum coverage and nucleotide identity of 86% and 96%, respectively (Table 1). A minimal ICE backbone, composed of CDS1, CDS3, CDS5, CDS14, CDS16, CDS17, CDS19, and CDS22 as previously defined (11), was detected in six STs (b to g), which is 28% (10 of 36) of the genomes. CDS1 was the most represented and was absent from only five isolates that clustered into three closely related STs, namely, h, i, and j (Table 1). Overall, the isolates could be divided into four groups: one that perfectly matched ST a as defined by WGS-SNP (Fig. 3), with isolates having only two CDSs, CDS1 and CDS22, and three other groups that displayed a combination of three (CDS16, 17 and 19), four (CDS14, 16, 17 and 19), or seven CDSs (CDSs 3, 5, 14, 16, 17, 19, and 22), respectively, and with or without CDS1. Overall, the distribution of ICE CDSs was consistent with the phylogenetic relationship of the strains, and as expected, there was no apparent relationship with their epidemiological background. Of the five isolates with a circularized genome, J81 (ST a), J228/279 (ST b), J137 (ST c), and J6 (ST l) (Fig. 4), only three, J137 and J228/279, had a complete ICEB-1 with organization similar to that of ICEB-1<sub>PG45</sub>, except for an IS element interrupting CDS23 in both (Fig. S2). ICEB-2 also occurred in the circularized isolates (Fig. 4) but none that perfectly matched the reference ICEB-2<sub>PG45</sub> (Fig. S3), and both ICEB-1 and ICEB-2 were found in all isolates (Fig. 4). Of note, all ICEs forms detected in these isolates were associated with one or more ISs, located either within the ICEs or at one extremity (Fig. S3).

Overall, MGEs, such as ICEs, MAgV1-like prophages, and ISs, were widespread among *M. bovis* strains circulating in Spain (Table 1). There was no correlation between the distribution of these elements and the epidemiological background of the isolates. MGEs' different genomic locations in closely related isolates and sequence conservation suggest that most MGEs are active within the *M. bovis* species and thus constitute a source for genetic diversification.

***M. bovis* isolates with a complex phylogenetic origin have a mosaic genome structure.** The inconsistent phylogenetic allocation of J137 and J228/J279 suggested that these isolates may have a mosaic genome structure with some of their chromosomal regions originating from different parental isolates. To test this hypothesis, comparative genomic studies were performed with these three isolates and one representative genome of each main branch as potential parents. Isolates J81 and J6 were chosen as representative genomes of branches A and B, respectively (Fig. 3), and were used to detect mosaic fragments in J137. Briefly, J137 reads were mapped onto the J81 genome, and those with mismatches were aligned to the J6 genome. Of these, reads perfectly matching the J6 genome were retained (Fig. 6A). The data revealed that J137 displayed a J81 chromosomal backbone with 27 fragments (0.5 to 6.8 kb) identical to J6, which represent about 5.4% of the genome (Table 2 and Data Set S2). One of these fragments included *polC*, explaining the inconsistencies observed with the phylogenetic trees based on this gene. As an internal control, J228 and J279 having similar genomic sequences (see above) but a slightly different sequence coverage (Table S1) were analyzed independently and shown to have a mosaic genome composed of a J81 backbone and 38 fragments identical to J6 encompassing about 7.1% of each genome (Table 2). Using this strategy, genomes from branch A were further analyzed, and 13 additional mosaic genomes belonging to the phylogenetic STs d to k were identified. These genomes were characterized by a J81 backbone with 5 to 39 fragments identical to J6 (Table 2 and Fig. 6B). As expected, our approach did not detect any fragment potentially transferred in isolates of the phylogenetic ST a because of the parental reference J81 also belonging to this ST.

Overall, up to 16 isolates of branch A were found to carry chromosomal fragments identical to J6 (branch B) and different from J81 (branch A). These mosaic genomes have acquired at least 5 to 39 fragments from a member or an ancestor of branch B, the sizes of



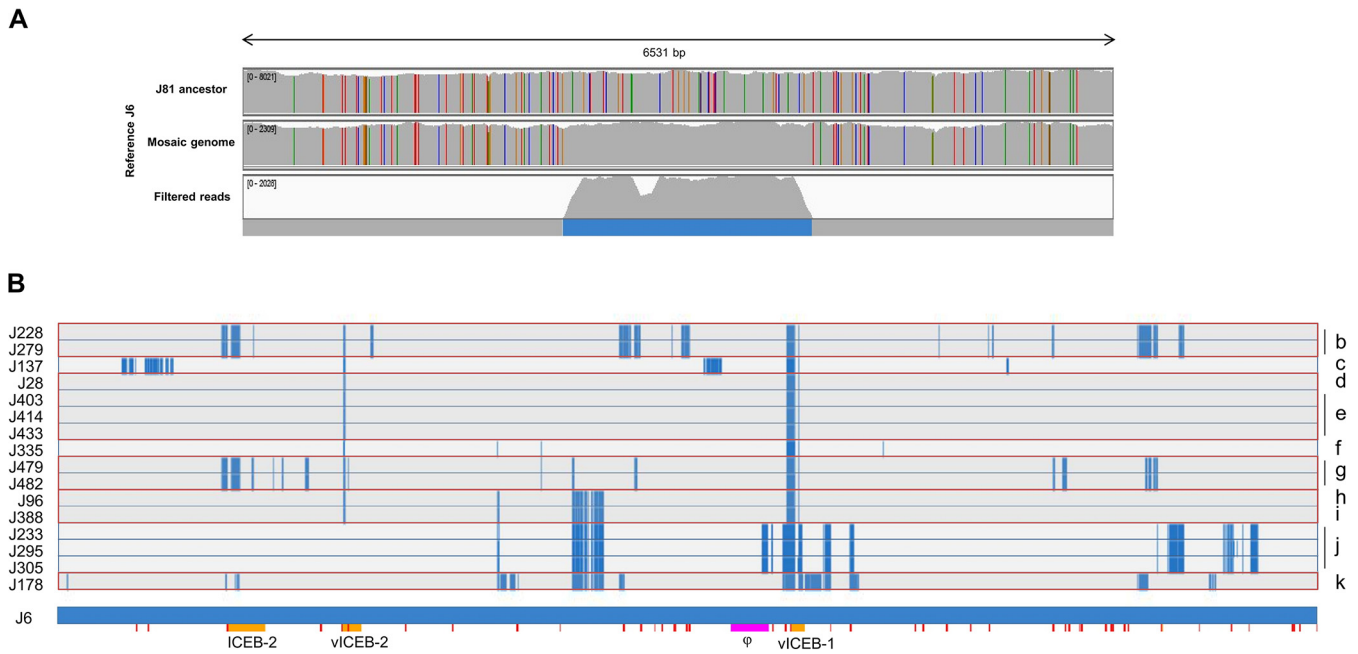


**FIG 6** Mosaic genomes identified in *M. bovis* isolates of branch A. (A) Visualization of a transferred fragment in mycoplasma mosaic genomes using IGV 2.7.0 (57). Illumina reads were aligned to the J6 circularized genome (branch B). First row, branch A hypothetical ancestor (J81); second row, mosaic genome (J137); third row, J137 reads filtered as different from J81 and identical to J6. Each color bar represents a SNP. The overall genotype of the mosaic genome is represented in the line below the alignments, with the genomic regions identical to J6 and J81 in blue and gray, respectively. (B) Fragments of branch B origin identified in branch A isolates are represented: J6-specific (branch B) and J81-specific (branch A) sequences are indicated in blue and gray, respectively. ICEs and MAgV1-like relative positions in the J6 genome are indicated by orange and pink fragments, respectively.

which ranged from 0.5 to 10.6 kb, and represented about 0.9 to 8.5% of the genomes (Table 2 and Data Set S2). As shown in Fig. 6B, at least eight different mosaic genomes were identified each corresponding to a different ST, except for d and e, and h and i, which could not be distinguished. Close examination of transferred fragments showed that gene exchanges affected, for instance, several housekeeping genes like *gpsA*, *polC*, *gltX*, *pta-2*, *tufA*, or *tkt* that are used

**TABLE 2** Chromosomal fragments of branch A isolates potentially acquired from branch B

Isolate	WGS-SNP ST	No. of fragments	Percentage of genome <sup>a</sup>
J81	a	-	-
J69	a	0	0
J72	a	0	0
J115	a	0	0
J131	a	0	0
J228	b	38	7.1
J279	b	38	7.1
J137	c	27	5.4
J28	d	5	0.9
J403	e	5	0.9
J414	e	5	0.9
J433	e	5	0.9
J335	f	6	1.1
J479	g	33	4.9
J482	g	32	4.9
J96	h	17	3.2
J388	i	17	3.2
J233	j	38	7.9
J295	j	39	8.1
J305	j	38	8
J178	k	36	8.5

<sup>a</sup>The percentage was estimated by the total size of the fragments identical to J6 (branch B) and absent from J81 (branch A) divided by the size of the J6 genome (see Data Set S2 for details of fragments positions for each isolate).

for typing (22–24), as well as accessory putative lipoproteins and membrane proteins. Of note, fragments identified as being exchanged also included ICEs or part of ICEs. Whether these originated from chromosomal transfer or ICE self-transmission is not known because both events have been documented in previous studies using *M. agalactiae* (12, 14, 15).

## DISCUSSION

By documenting the concomitant occurrence of two distinct mechanisms of HGT in field isolates of *M. bovis*, this study provides new insights into the evolution of pathogenic mycoplasma species in their natural host. Indeed, in addition to the classical horizontal transfer of MGEs, we provide evidence that MCT can take place in the field, most likely during coinfections by multiple strains. Although these events are expected to occur at low frequency, their impact is responsible for genome-wide diversity and reorganization within the *M. bovis* species, which in turn may compromise both diagnostic and disease control, as further discussed.

MLST data indicated the circulation of multiple *M. bovis* STs in Spanish cattle from 2016 to 2018. Phylogenetic tree reconstruction based on WGS-SNP genotyping further divided these isolates into two main branches, with branch A showing a greater level of intrastrain diversity than branch B. This was particularly true for MGEs, whose repertoire, distribution, and location were more variable, as illustrated by MagV1-like prophage sequences. The MagV1 prophage was initially reported in the genome of atypical *M. agalactiae* strains associated with a mortality episode in Alpine ibexes in France (26). As evidenced in this study, this phage also circulates in *M. bovis*, and the detection of a complete prophage sequence or vestigial forms at chromosomal position 536074 (PG45 numbering) in a majority of Spanish isolates (94%) suggested an early viral attack, most likely in a common ancestor of the two branches. Although a complete copy remained at this locus in most isolates of branch B, it was lost in two collected the same year in distinct geographical areas. Whether these originated from a single strain introduced in two distinct farms cannot be formally addressed, but their identical ICE pattern, which differed from the rest of branch B, argues in favor of this hypothesis.

The situation was more complex in branch A, in which complete MagV1-like copies also occurred in addition to vestigial or truncated forms but at different chromosomal positions, at either nucleotide 548254 or 911138. Altogether, these data indicate that three independent genetic events have occurred after the splitting of the two branches. These are (i) the excision of the prophage resulting in virus-free isolates (branch B), (ii) a new viral attack that targeted two distinct loci (branch A), and (iii) the viral erosion or truncation of the copy vertically inherited (branch A). Remarkably, the MagV1-like prophage sequence appeared to be highly stable in *M. bovis*, with 99% of nucleotide identity (more than 97% of the prophage sequence) in between the Spanish isolates and the Japanese strain KG4397 (AP019558). This suggests that the MagV1-like phage, which actively circulates in *M. bovis*, is under strong selection pressure. Whether this virus provides *M. bovis* with particular virulence or biological properties is unknown, and many of its CDSs remain hypothetical, without any associated functions. Phages are not restricted to *M. bovis* or its close relative *M. agalactiae* but were detected in many other bovine mycoplasma species, such as *M. alkalescens*, *M. bovis- genitalium*, *M. bovirhinis*, and *M. arginini*, with the latter species being able to also infect a wide range of hosts in addition to ruminants (27).

Detailed genetic analyses also predicted the occurrence of single or multiple copies of entire and vestigial ICEs, with again more complex ICE patterns in branch A. Whether the entire ICEs described here are fully functional needs to be formally demonstrated, but evidence for MCT supports this hypothesis. Indeed, mycoplasma ICEs are self-transmissible elements whose horizontal dissemination is not linked to MCT, yet MCT was shown to rely on the presence of functional ICE in at least one partner (11, 14). ISs were also highly widespread among contemporary Spanish isolates and contribute together with other MGEs to genome plasticity by relocating themselves, disrupting genes or promoting genome rearrangements (31). Hence, several ICEs and MAGV1-like CDSs were interrupted by ISs (Fig. 5 and Fig. S2 and

S3), and major chromosome inversions were detected between strains J6 (branch B), J81, and J137 (branch A) that could be associated with MGE located nearby.

Discrepancies in phylogenetic tree reconstruction when using different typing methods raised the question of whether MCT could explain this result. MCT is an atypical, conjugative process of HGT documented for *M. agalactiae* under laboratory conditions. Because MCT involves any region of the genome that can be transferred alone or in combination, this phenomenon does not conform to canonical Hfr/*oriT* models of chromosomal transfer and results in progenies composed of a variety of mosaic genomes, each being unique. In-depth comparative genome analyses were performed between a selection of Spanish *M. bovis* isolates of branch A, in which a higher genetic diversity was observed, and one representative from each branch as potential parents revealed the circulation of several distinct mosaic genomes. More specifically, data showed the exchange of 5 to 39 fragments (0.9 to 8.5% of the *M. bovis* genome) in between isolates of branches A and B. Our approach has several limits, and these data might underestimate the total amount of DNA exchanges because they do not detect silent events resulting from the exchange of fragments with identical sequences. In addition, the exact parents are not known and might not even have been collected in this study. Nevertheless, comparative genomic data were consistent with our MCT model (11) and thus strongly argue for the occurrence of MCT events in *M. bovis* that have generated viable mosaic genomes currently circulating in the field.

Spanish isolates were associated with genomic STs already reported in various parts of the world, suggesting a possible role for animal trading in the introduction of *M. bovis* strains in Spain, followed by an efficient transmission, circulation, and maintenance among and within the herds. Such a situation likely reflects animal movements between farms, a common practice in Spain (21). However, the genome mosaicism of several isolates also points toward MCT as an alternative cause for genetic diversity. When and where this phenomenon took place is unknown, and although this is probably not an isolated event, the frequency at which it occurs *in vivo* remains to be addressed. Interestingly, three animals turned out to be infected by two distinct isolates, one belonging to branch A and the other belonging to branch B (Table 1). Because isolates from both branches were recovered from the same farms on several occasions, this raised the question of whether this observation is due to the independent introduction of two distinct isolates or reflects the occurrence of MCT within the host, an exciting hypothesis that remains to be demonstrated.

As illustrated here with MLST, MCT may have a tremendous impact on epidemiological studies. In mosaic genomes of branch A, the exchange of at least one housekeeping gene was detected, including some used in *M. bovis*-specific MLST systems (22–24). These typing systems enable the characterization of *M. bovis* population structure and are used to trace the history and geographic route of dissemination of the pathogen. Hence, abrupt replacement of housekeeping genes by MCT could reduce the epidemiological value of MLST, because the variety of STs described in a given country, region, or farm may be not only the result of importing foreign strains but also the result of recombination between autochthonous strains. On the other hand, species-specific diagnosis may also be affected by MCT because many other mycoplasma species share the same ecological niche with *M. bovis* in cattle (14, 32, 33). Indeed, several studies pointed toward the ability of different species to engage in MCT. Indeed, MCT has been documented under laboratory conditions between *M. bovis* and *M. agalactiae* (14), and *in silico* data showed that *M. agalactiae* has exchanged a large portion of its genome with phylogenetically remote ruminant mycoplasma species of the mycoides cluster (6). Thus, MCT by altering the boundaries between species and strains may impact diagnostic studies in addition to epidemiological studies, a situation that may compromise the implementation of efficient control strategies. Putative membrane lipoproteins and membrane proteins were encoded on other transferred fragments. Because mycoplasmas lack the cell wall, the membrane is in direct contact with the host, and modification, gain, or loss of this type of gene may drastically affect the host-pathogen interaction (34).

MCT may also compromise disease treatment. In *M. agalactiae*, MCT was shown to act as an accelerator of fluoroquinolone (FLQ) resistance dissemination *in vitro* under enrofloxacin-selective pressure (16). Faucher et al. showed that MCT provided susceptible mycoplasma

strains with the ability to rapidly acquire from preexisting resistant populations, multiple chromosomal loci carrying antimicrobial mutations in *gyrA*, *parE*, and *parC* genes (16). In Spain, circulating *M. bovis* isolates are resistant to macrolides, lincosamides, and tetracyclines (21). However, although isolates in branch B were all susceptible to FLQ, most isolates found in branch A have acquired resistance-associated mutations. A single event of MCT, from FLQ-resistant to FLQ-susceptible isolates, followed by the expansion and transmission of the FLQ-resistant mosaic genome to other animals, farms or regions, may definitively compromise treatment of *M. bovis* infections with FLQ. Indirectly, animal movements between farms, a common practice in the Spanish beef cattle industry, would likely contribute to this situation by providing a means for mixing isolates with different antibiotic susceptibilities (21).

The high level of genetic diversity documented for branch A was consistent with previous observations showing a higher ability of *polC*-ST3 isolates to acquire mutations in the quinolone resistance-determining regions (QRDR) and develop resistance under selective pressure (35). The apparent selective advantage exhibited by branch A raises questions regarding the simultaneous circulation of another phylogenetic branch with limited genetic diversity. Other studies reported decreasing diversity and monoclonal spread in several countries (22, 36–38). The existence of lineages with a high level of genetic diversity and others with low diversity has been described on a worldwide scale (39, 40). This situation is not limited to *M. bovis* and has been observed in other mycoplasmas like in small ruminants with *M. agalactiae* (41, 42), for which ovine isolates are described as more clonal, whereas caprine are more variable (43). In *M. bovis*, no correlation with host type or age was revealed. Our study highlights that the coexistence of lineages at the herd level and even at the animal level enables events of HGT like MCT. The occurrence, extension, and evolution of this phenomenon have to be explored and integrated in control and diagnosis based on genomic typing.

## MATERIALS AND METHODS

**Mycoplasma sequences, genome *de novo* assembly, and annotation.** Genome sequences of *M. bovis* reference strain PG45 (CP002188.1), RM16, and representative field isolates *polC*-ST2 ( $n = 16$ ) and *polC*-ST3 ( $n = 20$ ) collected between 2016 and 2018 in Spain were included in this study. The geographic and anatomic origins of the isolates at the time samples were collected are summarized in Table 1. These isolates were obtained in a previous study and sequenced using Illumina technology HiSeq (paired-end,  $2 \times 150$  bp) (21). WGS reads were retrieved from the European Nucleotide Archive (ENA) database (PRJEB38707). Bioinformatic analyses were conducted on the Galaxy platform (Genotoul, Toulouse, France). The quality of the sequencing reads was analyzed with the FastQC tool (<https://www.bioinformatics.babraham.ac.uk/projects/fastqc/>). *De novo* assemblies were obtained with Unicycler (44). Circular genomes were obtained for five isolates identified as MCT potential parents or progenies by combining Illumina reads (see above) with long reads produced by Oxford Nanopore sequencing technology using *M. bovis* genomic DNA extracted with the phenol-chloroform method (45). This approach was also used to circularize the genome of strain RM16 (27, 28). For all genome assemblies obtained, contigs with less than 200 bp were excluded, validated with QUAST (46), and annotated with Prokka (47). Annotated files were visualized with Artemis 16.0.0 (48) and Artemis comparison tool (ACT 17.0.1) (49). Assembly metrics are available in Table S1. Average nucleotide identity (ANI) was calculated pairwise between assemblies of 36 Spanish isolates with FastANI-1.2 (50) (Data Set S1).

**Phylogenetic analysis of isolates.** The phylogenetic relationships among the isolates were approached by tree reconstruction based on gene sequences of different MLST schemes and by WGS-SNP analyses. Two MLST systems referred in the text to as MLST-1 (23) and MLST-2 (24) were used. Characterization with MLST-1 was based on the analysis of the partial sequences of the *dnaA*, *metS*, *recA*, *tufA*, *atpA*, *rpoD*, and *tkt* genes (23). The amplicon sequences of these housekeeping genes were extracted from the annotated assemblies using Artemis 16.0.0 (48) and MLST primer sequences. They were trimmed to the analysis sequence size using MEGA X (51), and allelic profiles were assigned by blast comparison with the different allele sequences of each gene included in MLST-1 (23, 39, 52). New STs and allele sequences are provided in Tables S2 and S3. Typing with the MLST-2 was based on the analysis of the partial sequences of *dnaA*, *gltX*, *gpsA*, *gyrB*, *pta-2*, *tdk*, and *tkt* (24). The STs were assigned with PubMLST database (automated sequence query for data derived from genome assemblies, [https://pubmlst.org/bigsub?db=pubmlst\\_mbovis\\_seqdef](https://pubmlst.org/bigsub?db=pubmlst_mbovis_seqdef)). New ST profiles obtained with MLST-2 were submitted to the public database PubMLST. Concatenated nucleotide sequences of each MLST system were used to reconstruct phylogenetic trees in MEGA X (51). The trees were constructed with the neighbor-joining method, the Tamura-Nei genetic distance model, and 1,000 bootstrap replications.

The WGS-SNP-based analysis was performed by comparing the genome Illumina assemblies with PG45 genome (CP002188.1) as a reference on CSI phylogeny webserver (53) using parameters as previously described (54). Contigs of less than 1,000 nucleotides were excluded. SNPs matrices generated by the server were used to create a phylogenetic tree using MEGA X (51). The tree was constructed with the maximum likelihood method, the Tamura-Nei genetic distance model, and 1,000 bootstrap replications. A letter was manually assigned to each ST of isolates based on tree branches.

**Analysis of the global population structure of *M. bovis*.** A minimum spanning tree (MST) that illustrates the ST distribution of isolates identified in this and other studies was created with GrapeTree (55). Isolates registered with an assigned ST in the PubMLST database (<https://pubmlst.org/organisms/mycoplasma-bovis>) (MLST-2) as of January 2020 were included.

**Reconstruction of the mosaic genomes.** The identification of strains with mosaic genomes and their hypothetical ancestors was based on the analysis of the phylogenetic trees. The short paired-end reads of possible isolates with mosaic genomes were mapped to the hypothetical ancestor's genomes by using BWA-MEM (56). The alignments were visualized with the Integrative Genome Viewer (IGV 2.7.0) (57). Reconstruction of the mosaic genomes was performed by "donor" specific reads detection as explained by Faucher et al. (16) and Dordet-Frisoni et al. (15). Reads of possible mosaic genomes were aligned on the "recipient" genome, reads with mismatch were recovered and then aligned to the donor genome. Donor specific reads were visualized in IGV 2.7.0 (57) and manually curated by using Artemis 16.0.0 and the Artemis BamView (48), and only reads with coverage higher than 50× and feature size higher than 500 bp were considered. False-positive fragments (also present in the negative control recipient ancestor), fragments present in the duplicated *rm* operon, and fragments having no SNPs based on Bam files were manually curated. Fragment plots were visualized with the Artemis 16.0.0 DNA plotter tool (48).

Additionally, the genome of three strains with mosaic genomes, namely J137, J228, and J279, was further circularized as described above. The effectiveness of the filtering process was then checked by mapping the paired-end reads of both hypothetical ancestors (donor and recipient) on the circularized genome of mosaic genomes and visualizing that, in the transferred regions, there were no SNPs in the alignment donor-mosaic genome but many SNPs in the alignment recipient-mosaic genome.

**Detection of MGE: ICEs, MAgV1-like phage, and ISs.** ICEs sequence detection was done by comparative analyses with the reference strain PG45 (CP002188.1), which carries two copies of ICE: ICEB-1 and ICEB-2 (30). The ICE backbone CDSs sequences 3, 5, 14, 16, 17, 19, and 22 of the ICEB-1 and the CDS1 sequence, which is only present in the ICEB-2 (GenBank locus tags: MBOVPG45\_0495 [CDS3], MBOVPG45\_0494 [CDS5], MBOVPG45\_0487 [CDS14], MBOVPG45\_0484 [CDS16], MBOVPG45\_0483 [CDS17], MBOVPG45\_0481 [CDS19], MBOVPG45\_0479 [CDS22], and MBOVPG45\_0213 [CDS1]), were used as queries for BLASTn search against assemblies of the genomes studied.

Phage sequences were searched with MAgV1-like phage of *M. bovis* strain RM16 as reference, because it carries one copy of the phage (27, 28). Comparative analyses with PG45, which lacks the phage sequence, permitted the determination of the phage insertion point. Finally, the presence of ISs was investigated by searches against the ISFinder database (29).

**Data availability.** Nucleotide sequence assemblies were submitted to GenBank and are available under the following accession numbers: CP068734 (J6), JAERV1000000000 (J28), JAERVH0000000000 (J69), JAERVG0000000000 (J72), CP068733 (J81), JAERVF0000000000 (J96), JAERVE0000000000 (J103), JAERVD0000000000 (J115), JAERVCO0000000000 (J131), JAERVB0000000000 (J136), CP068732 (J137), JAERVA0000000000 (J175), JAERUZ0000000000 (J178), JAERUY0000000000 (J226), CP068731 (J228), JAERUX0000000000 (J233), JAERUW0000000000 (J276), CP068730 (J279), JAERUV0000000000 (J295), JAERUU0000000000 (J305), JAERUT0000000000 (J319), JAERUS0000000000 (J330), JAERUR0000000000 (J335), JAERUQ0000000000 (J336), JAERUP0000000000 (J341), JAERUO0000000000 (J356), JAERUN0000000000 (J368), JAERUM0000000000 (J377), JAERUL0000000000 (J388), JAERUK0000000000 (J391), JAERUJ0000000000 (J403), JAERUI0000000000 (J410), JAERUH0000000000 (J414), JAERUG0000000000 (J433), JAERUF0000000000 (J479), JAERUE0000000000 (J482), and CP077758 (RM16). The raw FastQ reads used for mosaic genome reconstruction are available at the EMBL database, the European Nucleotide Archive (ENA) at <http://www.ebi.ac.uk/ena> under study accession number PRJEB38707.

## SUPPLEMENTAL MATERIAL

Supplemental material is available online only.

**SUPPLEMENTAL FILE 1**, PDF file, 0.5 MB.

**SUPPLEMENTAL FILE 2**, XLSX file, 0.02 MB.

**SUPPLEMENTAL FILE 3**, XLSX file, 0.02 MB.

## ACKNOWLEDGMENTS

We are grateful to the Genotoul bioinformatics platform Toulouse Midi-Pyrenees for providing help and storage resources. This research was supported by the Spanish Ministry of Economy and Competitiveness (Spanish Government) cofinanced by FEDER funds (project AGL2016-76568-R) and financial support from the INRAE and ENVT. Ana García-Galán Pérez is a beneficiary of research fellowship BES-2017-080186 from the state subprogram training of the State Program for the Promotion of Talent and Its Employability.

## REFERENCES

- Ochman H, Lawrence JG, Groisman EA. 2000. Lateral gene transfer and the nature of bacterial innovation. *Nature* 405:299–304. <https://doi.org/10.1038/35012500>.
- Razin S, Yogev D, Naot Y. 1998. Molecular biology and pathogenicity of mycoplasmas. *Microbiol Mol Biol Rev* 62:1094–1156. <https://doi.org/10.1128/MMBR.62.4.1094-1156.1998>.



3. Sirand-Pugnet P, Citti C, Barré A, Blanchard A. 2007. Evolution of *Mollicutes*: down a bumpy road with twists and turns. *Res Microbiol* 158:754–766. <https://doi.org/10.1016/j.jresmic.2007.09.007>.
4. Teachman AM, French CT, Yu H, Simmons WL, Dybvig K. 2002. Gene transfer in *Mycoplasma pulmonis*. *J Bacteriol* 184:947–951. <https://doi.org/10.1128/jb.184.4.947-951.2002>.
5. Vasconcelos ATR, Ferreira HB, Bizarro CV, Bonatto SL, Carvalho MO, Pinto PM, Almeida DF, Almeida LGP, Almeida R, Alves-Filho L, Assunção EN, Azevedo VAC, Bogo MR, Brigido MM, Brocchi M, Burity HA, Camargo AA, Camargo SS, Carepo MS, Carraro DM, de Mattos Cascardo JC, Castro LA, Cavalcanti G, Chemale G, Collevatti RG, Cunha CW, Dallagiovanna B, Dambrós BP, Dellagostin OA, Falcão C, Fantinatti-Garboggini F, Felipe MSS, Fiorentin L, Franco GR, Freitas NSA, Frías D, Grangeiro TB, Grisard EC, Guimarães CT, Hungria M, Jardim SN, Krieger MA, Laurino JP, Lima LFA, Lopes MI, Loreto ELS, Madeira HMF, Manfio GP, Maranhão AQ, Martinkovics CT, Medeiros SRB, Moreira MAM, Neiva M, Ramalho-Neto CE, Nicolás MF, Oliveira SC, Paixão RFC, et al. 2005. Swine and poultry pathogens: the complete genome sequences of two strains of *Mycoplasma hyopneumoniae* and a strain of *Mycoplasma synoviae*. *J Bacteriol* 187:5568–5577. <https://doi.org/10.1128/JB.187.16.5568-5577.2005>.
6. Sirand-Pugnet P, Lartigue C, Marendra M, Jacob D, Barré A, Barbe V, Schenowitz C, Mangenot S, Couloux A, Segurens B, de Daruvar A, Blanchard A, Citti C. 2007. Being pathogenic, plastic, and sexual while living with a nearly minimal bacterial genome. *PLoS Genet* 3:e75. <https://doi.org/10.1371/journal.pgen.0030075>.
7. Pereyre S, Sirand-Pugnet P, Beven L, Charron A, Renaudin H, Barré A, Avenaud P, Jacob D, Couloux A, Barbe V, de Daruvar A, Blanchard A, Bébéar C. 2009. Life on arginine for *Mycoplasma hominis*: clues from its minimal genome and comparison with other human urogenital mycoplasmas. *PLoS Genet* 5:e1000677. <https://doi.org/10.1371/journal.pgen.1000677>.
8. Xiao L, Paralanov V, Glass JI, Duffy LB, Robertson JA, Cassell GH, Chen Y, Waites KB. 2011. Extensive horizontal gene transfer in ureaplasmas from humans questions the utility of serotyping for diagnostic purposes. *J Clin Microbiol* 49:2818–2826. <https://doi.org/10.1128/JCM.00637-11>.
9. Lo W-S, Gasparich GE, Kuo C-H. 2015. Found and lost: the fates of horizontally acquired genes in arthropod-symbiotic spiroplasma. *Genome Biol Evol* 7:2458–2472. <https://doi.org/10.1093/gbe/evv160>.
10. Torres-Puig S, Martínez-Torró C, Granero-Moya I, Querol E, Piñol J, Pich OQ. 2018. Activation of  $\sigma$ 20-dependent recombination and horizontal gene transfer in *Mycoplasma genitalium*. *DNA Res* 25:383–393. <https://doi.org/10.1093/dnares/dsy011>.
11. Citti C, Dordet-Frisoni E, Nouvel LX, Baranowski E. 2018. Horizontal gene transfers in mycoplasmas (*Mollicutes*). *Curr Issues Mol Biol* 29:3–22. <https://doi.org/10.21775/cimb.029.003>.
12. Dordet-Frisoni E, Marendra MS, Sagné E, Nouvel LX, Guérrillot R, Glaser P, Blanchard A, Tardy F, Sirand-Pugnet P, Baranowski E, Citti C. 2013. ICEA of *Mycoplasma agalactiae*: a new family of self-transmissible integrative elements that confers conjugative properties to the recipient strain. *Mol Microbiol* 89:1226–1239. <https://doi.org/10.1111/mmi.12341>.
13. Baranowski E, Dordet-Frisoni E, Sagné E, Hygonenq MC, Pretre G, Claverol S, Fernandez L, Nouvel LX, Citti C. 2018. The integrative conjugative element (ICE) of *Mycoplasma agalactiae*: fey elements involved in horizontal dissemination and influence of coresident ICEs. *mBio* 9:e00873-18. <https://doi.org/10.1128/mBio.00873-18>.
14. Dordet-Frisoni E, Sagné E, Baranowski E, Breton M, Nouvel LX, Blanchard A, Marendra MS, Tardy F, Sirand-Pugnet P, Citti C. 2014. Chromosomal transfers in mycoplasmas: when minimal genomes go mobile. *mBio* 5:e01958-14. <https://doi.org/10.1128/mBio.01958-14>.
15. Dordet-Frisoni E, Faucher M, Sagné E, Baranowski E, Tardy F, Nouvel LX, Citti C. 2019. Mycoplasma chromosomal transfer: a distributive, conjugative process creating an infinite variety of mosaic genomes. *Front Microbiol* 10:2441. <https://doi.org/10.3389/fmicb.2019.02441>.
16. Faucher M, Nouvel LX, Dordet-Frisoni E, Sagné E, Baranowski E, Hygonenq M-C, Marendra MS, Tardy F, Citti C. 2019. Mycoplasmas under experimental antimicrobial selection: the unpredicted contribution of horizontal chromosomal transfer. *PLoS Genet* 15:e1007910. <https://doi.org/10.1371/journal.pgen.1007910>.
17. Tardy F, Mick V, Dordet-Frisoni E, Marendra MS, Sirand-Pugnet P, Blanchard A, Citti C. 2015. Integrative conjugative elements are widespread in field isolates of mycoplasma species pathogenic for ruminants. *Appl Environ Microbiol* 81:1634–1643. <https://doi.org/10.1128/AEM.03723-14>.
18. Nicholas RAJ, Ayling RD. 2003. *Mycoplasma bovis*: disease, diagnosis, and control. *Res Vet Sci* 74:105–112. [https://doi.org/10.1016/S0034-5288\(02\)00155-8](https://doi.org/10.1016/S0034-5288(02)00155-8).
19. Maunsell FP, Woolums AR, Francoz D, Rosenbusch RF, Step DL, Wilson DJ, Janzen ED. 2011. *Mycoplasma bovis* infections in cattle. *J Vet Intern Med* 25:772–783. <https://doi.org/10.1111/j.1939-1676.2011.0750.x>.
20. Gille L, Evrard J, Callens J, Supré K, Grégoire F, Boyen F, Haesebrouck F, Deprez P, Pardon B. 2020. The presence of *Mycoplasma bovis* in colostrum. *Vet Res* 51:54. <https://doi.org/10.1186/s13567-020-00778-w>.
21. García-Galán A, Nouvel LX, Baranowski E, Gómez-Martín Á, Sánchez A, Citti C, de la Fe C. 2020. *Mycoplasma bovis* in Spanish cattle herds: two groups of multiresistant isolates predominate, with one remaining susceptible to fluoroquinolones. *Pathogens* 9:545. <https://doi.org/10.3390/pathogens9070545>.
22. Becker CAM, Thibault FM, Arcangioli M-A, Tardy F. 2015. Loss of diversity within *Mycoplasma bovis* isolates collected in France from bovines with respiratory diseases over the last 35 years. *Infect Genet Evol* 33:118–126. <https://doi.org/10.1016/j.meegid.2015.04.019>.
23. Rosales RS, Churchward CP, Schnee C, Sachse K, Lysnyansky I, Catania S, Lob L, Ayling RD, Nicholas RAJ. 2015. Global multilocus sequence typing analysis of *Mycoplasma bovis* isolates reveals two main population clusters. *J Clin Microbiol* 53:789–794. <https://doi.org/10.1128/JCM.01910-14>.
24. Register KB, Lysnyansky I, Jelinski MD, Boatwright WD, Waldner M, Bayles DO, Pilo P, Alt DP. 2020. Comparison of two multilocus sequence typing schemes for *Mycoplasma bovis* and revision of the PubMLST reference method. *J Clin Microbiol* 58:e00283-20. <https://doi.org/10.1128/JCM.00283-20>.
25. Röske K, Foecking MF, Yooseph S, Glass JI, Calcutt MJ, Wise KS. 2010. A versatile palindromic amphipathic repeat coding sequence horizontally distributed among diverse bacterial and eucaryotic microbes. *BMC Genomics* 11:430. <https://doi.org/10.1186/1471-2164-11-430>.
26. Tardy F, Baranowski E, Nouvel LX, Mick V, Manso-Silván L, Thiaucourt F, Thébault P, Breton M, Sirand-Pugnet P, Blanchard A, Garnier A, Gilbert P, Game Y, Poumarat F, Citti C. 2012. Emergence of atypical *Mycoplasma agalactiae* strains harboring a new prophage and associated with an alpine wild ungulate mortality episode. *Appl Environ Microbiol* 78:4659–4668. <https://doi.org/10.1128/AEM.00332-12>.
27. Citti C, Baranowski E, Dordet-Frisoni E, Faucher M, Nouvel LX. 2020. Genomic islands in mycoplasmas. *Genes* 11:836. <https://doi.org/10.3390/genes11080836>.
28. Zhu X, Dordet-Frisoni E, Gillard L, Ba A, Hygonenq M-C, Sagné E, Nouvel LX, Maillard R, Assié S, Guo A, Citti C, Baranowski E. 2019. Extracellular DNA: a nutritional trigger of *Mycoplasma bovis* cytotoxicity. *Front Microbiol* 10:2753. <https://doi.org/10.3389/fmicb.2019.02753>.
29. Siguier P, Perochon J, Lestrade L, Mahillon J, Chandler M. 2006. ISfinder: the reference centre for bacterial insertion sequences. *Nucleic Acids Res* 34:D32–D36. <https://doi.org/10.1093/nar/gkj014>.
30. Wise KS, Calcutt MJ, Foecking MF, Röske K, Madupu R, Methé BA. 2011. Complete genome sequence of *Mycoplasma bovis* type strain PG45 (ATCC 25523). *Infect Immun* 79:982–983. <https://doi.org/10.1128/IAI.00726-10>.
31. Marendra SM. 2014. Genomic mosaics, p 15–54. In Browning GF, Citti C (ed), *Mollicutes: molecular biology and pathogenesis*. Caister Academic Press, Norfolk, UK.
32. Thomas A, Ball H, Dizier I, Trolin A, Bell C, Mainil J, Linden A. 2002. Isolation of mycoplasma species from the lower respiratory tract of healthy cattle and cattle with respiratory disease in Belgium. *Vet Rec* 151:472–476. <https://doi.org/10.1136/vr.151.16.472>.
33. Parker AM, Sheehy PA, Hazelton MS, Bosward KL, House JK. 2018. A review of mycoplasma diagnostics in cattle. *J Vet Intern Med* 32:1241–1252. <https://doi.org/10.1111/jvim.15135>.
34. Citti C, Nouvel LX, Baranowski E. 2010. Phase and antigenic variation in mycoplasmas. *Future Microbiol* 5:1073–1085. <https://doi.org/10.2217/fmb.10.71>.
35. Khalil D, Becker CAM, Tardy F. 2016. Alterations in the quinolone resistance-determining regions and fluoroquinolone resistance in clinical isolates and laboratory-derived mutants of *Mycoplasma bovis*: not all genotypes may be equal. *Appl Environ Microbiol* 82:1060–1068. <https://doi.org/10.1128/AEM.03280-15>.
36. Bürki S, Sperser J, Bodmer M, Pilo P. 2016. A dominant lineage of *Mycoplasma bovis* is associated with an increased number of severe mastitis cases in cattle. *Vet Microbiol* 196:63–66. <https://doi.org/10.1016/j.vetmic.2016.10.016>.
37. Parker AM, Shukla A, House JK, Hazelton MS, Bosward KL, Kokotovic B, Sheehy PA. 2016. Genetic characterization of Australian *Mycoplasma bovis* isolates through whole genome sequencing analysis. *Vet Microbiol* 196:118–125. <https://doi.org/10.1016/j.vetmic.2016.10.010>.
38. Menghwar H, He C, Zhang H, Zhao G, Zhu X, Khan FA, Faisal M, Rasheed MA, Zubair M, Memon AM, Ridley A, Robertson ID, Chen Y, Guo A. 2017. Genotype distribution of Chinese *Mycoplasma bovis* isolates and their evolutionary relationship to strains from other countries. *Microb Pathog* 111:108–117. <https://doi.org/10.1016/j.micpath.2017.08.029>.

39. Tardy F, Aspan A, Autio T, Ridley A, Tricot A, Colin A, Pohjanvirta T, Smid B, Harders F, Lindegaard M, Tølbøll Lauritsen K, Lyhs U, Wisselink HJ, Strube ML. 2020. *Mycoplasma bovis* in nordic European countries: emergence and dominance of a new clone. *Pathogens* 9:875. <https://doi.org/10.3390/pathogens9110875>.
40. Kumar R, Register K, Christopher-Hennings J, Moroni P, Gioia G, Garcia-Fernandez N, Nelson J, Jelinski MD, Lysnyansky I, Bayles D, Alt D, Scaria J. 2020. Population genomic analysis of *Mycoplasma bovis* elucidates geographical variations and genes associated with host-types. *Microorganisms* 8:1561. <https://doi.org/10.3390/microorganisms8101561>.
41. McAuliffe L, Gosney F, Hlusek M, de Garnica ML, Spargser J, Kargl M, Rosengarten R, Ayling RD, Nicholas RAJ, Ellis RJ. 2011. Multilocus sequence typing of *Mycoplasma agalactiae*. *J Med Microbiol* 60:803–811. <https://doi.org/10.1099/jmm.0.028159-0>.
42. Nouvel LX, Marena MS, Glew MD, Sagne E, Giammarinaro P, Tardy F, Poumarat F, Rosengarten R, Citti C. 2012. Molecular typing of *Mycoplasma agalactiae*: tracing European-wide genetic diversity and an endemic clonal population. *Comp Immunol Microbiol Infect Dis* 35:487–496. <https://doi.org/10.1016/j.cimid.2012.04.005>.
43. De la Fe C, Amores J, Tardy F, Sagne E, Nouvel LX, Citti C. 2012. Unexpected genetic diversity of *Mycoplasma agalactiae* caprine isolates from an endemic geographically restricted area of Spain. *BMC Vet Res* 8:146. <https://doi.org/10.1186/1746-6148-8-146>.
44. Wick RR, Judd LM, Gorrie CL, Holt KE. 2017. Unicycler: resolving bacterial genome assemblies from short and long sequencing reads. *PLoS Comput Biol* 13:e1005595. <https://doi.org/10.1371/journal.pcbi.1005595>.
45. Sambrook J, Fritsch E, Maniatis T. 1989. *Molecular cloning: a laboratory manual*, 2nd ed. Cold Spring Harbor Laboratory Press, Cold Spring Harbor, NY.
46. Gurevich A, Saveliev V, Vyahhi N, Tesler G. 2013. QUAST: quality assessment tool for genome assemblies. *Bioinformatics* 29:1072–1075. <https://doi.org/10.1093/bioinformatics/btt086>.
47. Seemann T. 2014. Prokka: rapid prokaryotic genome annotation. *Bioinformatics* 30:2068–2069. <https://doi.org/10.1093/bioinformatics/btu153>.
48. Rutherford K, Parkhill J, Crook J, Horsnell T, Rice P, Rajandream MA, Barrell B. 2000. Artemis: sequence visualization and annotation. *Bioinformatics* 16:944–945. <https://doi.org/10.1093/bioinformatics/16.10.944>.
49. Carver TJ, Rutherford KM, Berriman M, Rajandream MA, Barrell BG, Parkhill J. 2005. ACT: the Artemis comparison tool. *Bioinformatics* 21:3422–3423. <https://doi.org/10.1093/bioinformatics/bti553>.
50. Goris J, Konstantinidis KT, Klappenbach JA, Coenye T, Vandamme P, Tiedje JM. 2007. DNA–DNA hybridization values and their relationship to whole-genome sequence similarities. *Int J Syst Evol Microbiol* 57:81–91. <https://doi.org/10.1099/ijs.0.64483-0>.
51. Kumar S, Stecher G, Li M, Knyaz C, Tamura K. 2018. MEGA X: molecular evolutionary genetics analysis across computing platforms. *Mol Biol Evol* 35:1547–1549. <https://doi.org/10.1093/molbev/msy096>.
52. Lysnyansky I, Freed M, Rosales RS, Mikula I, Khateb N, Gerchman I, van Straten M, Levisohn S. 2016. An overview of *Mycoplasma bovis* mastitis in Israel (2004–2014). *Vet J* 207:180–183. <https://doi.org/10.1016/j.tvjl.2015.10.057>.
53. Kaas RS, Leekitcharoenphon P, Aarestrup FM, Lund O. 2014. Solving the problem of comparing whole bacterial genomes across different sequencing platforms. *PLoS One* 9:e104984. <https://doi.org/10.1371/journal.pone.0104984>.
54. Yair Y, Borovok I, Mikula I, Falk R, Fox LK, Gophna U, Lysnyansky I. 2020. Genomics-based epidemiology of bovine *Mycoplasma bovis* strains in Israel. *BMC Genomics* 21:70. <https://doi.org/10.1186/s12864-020-6460-0>.
55. Zhou Z, Alikhan NF, Sergeant MJ, Luhmann N, Vaz C, Francisco AP, Carriço JA, Achtman M. 2018. GrapeTree: visualization of core genomic relationships among 100,000 bacterial pathogens. *Genome Res* 28:1395–1404. <https://doi.org/10.1101/gr.232397.117>.
56. Li H, Durbin R. 2009. Fast and accurate short read alignment with Burrows-Wheeler transform. *Bioinformatics* 25:1754–1760. <https://doi.org/10.1093/bioinformatics/btp324>.
57. Thorvaldsdóttir H, Robinson JT, Mesirov JP. 2013. Integrative Genomics Viewer (IGV): high-performance genomics data visualization and exploration. *Brief Bioinform* 14:178–192. <https://doi.org/10.1093/bib/bbs017>.
58. Hale HH, Helmboldt CF, Plastringer WN, Stula EF. 1962. Bovine mastitis caused by a mycoplasma species. *Cornell Vet* 52:582–591.
59. Madeira F, Mi Park Y, Lee J, Buso N, Gur T, Madhusoodanan N, Basutkar P, Tivey ARN, Potter SC, Finn RD, Lopez R. 2019. The EMBL-EBI search and sequence analysis tools APIs in 2019. *Nucleic Acids Res* 47:W636–W641. <https://doi.org/10.1093/nar/gkz268>.